

Ernest Agee*, Benjamin MacCall and Alexander Gluhovsky

Department of Earth and Atmospheric Sciences
Purdue University

1. INTRODUCTION

Advances in the large eddy simulation (LES) of certain meteorological flows continue today, as well as for a variety of sub-fields in engineering fluid mechanics. For an overview of issues and pertinent questions to be considered in LES, see Pope (2004) and Lesieur et al. (2005). Interestingly, the LES approach can be traced to the pioneering work of meteorologists (Smagorinsky 1963; Lilly 1967; and Deardorff 1974). Convective planetary boundary layers (PBLs) have been studied extensively from the initial efforts by Deardorff (1970, 1974, 1980) to subsequent studies by Moeng (1984, 1986), Moeng and Wyngaard (1988), Tripoli (1992), Moeng and Sullivan (1994), Rao and Agee (1996); Agee and Gluhovsky (1999), Mayor et al. (2003), hereafter referred to as MTE, Sorbjan (2004), and Zurn-Birkhimer et al. (2005), hereafter referred to as ZBAS. All of these convective PBL studies can be traced to versions of three different pedagogies of LES models: 1) NCAR, 2) Tripoli and 3) Sorbjan. Needless to say, others have made many contributions in LES, e.g., Schumann (1975, 1993), Mason (1989) and Nieuwstadt et al. (1991). This study has focused more specifically on the use of the Sullivan-NCAR LES code (hereafter referred to as SN-LES) to better understand the evolution of convective coherent structures (CS) that form within the PBL during cold air outbreaks (CAOs) over warmer water. The 13 January 1998 CAO during the Lake-Induced Convection Experiment (Lake-ICE) held over Lake Michigan has been the focus of two previous LES model studies of the convective PBL. These are with a) the Tripoli model (see Tripoli 1992) with results presented in MTE and b) the Sorbjan model (see Sorbjan 2004) with results presented in ZBAS. Each of these two model simulations of the Lake-ICE CAO has provided insight into the air mass transformation that typically occurs with such wintertime cold air outbreaks over warmer water. As both of these studies have shown, the Lake-ICE field data, and in particular the lidar data, have afforded a unique opportunity for making comparison between model data and field data. This study now brings into consideration yet a third LES model (the NCAR model, see, e.g., Moeng and Sullivan 1994) that has been initialized with the same CAO field data obtained during Lake-ICE. The objectives of this latest work are to make some comparisons between the convective patterns simulated by three popular LES models, noting agreements and differences. As

discussed by Pope (2004), no two LES models can be expected to produce the same computed fields. More importantly in this study has been the use of the SN-LES model to examine the spatial and temporal evolution of the convective CS that develop in the CFP region (between the Wisconsin shoreline and the cloud-topped PBL out over the lake). New findings for this CAO event show the formation of different scales of CS that originate at different levels (including the identification of the level where each CS is best defined) and how these structures evolve and grow (or weaken) at different levels with respect to time. It is argued that these results provide new insight into the manner of evolving convective structures, from near the lake surface through the entire boundary layer, and that this morphology can be labeled as a new paradigm for viewing convective organization in the marine PBL from the microscale to the mesoscale. The traditional view of thermal coalescence seems less evident than the proposed self-organization and energy transfer between coexisting length scales. The three microscale CS are best defined near the lake surface, while the two mesoscale CS are best defined in the mixed layer (even though both scales are prevalent for the entire runtime of the LES).

2. CONCEPTUAL PHYSICAL MODEL AT THE AIR-LAKE INTERFACE

The 13 January 1998 CAO in Lake-ICE has been observed to contain four different CS; three in the CFP region near the Wisconsin shoreline and an additional one in the cloud-topped PBL (see ZBAS). These four structures and their observed characteristic length scales are: CS1 (30m), CS2 (200m), CS3 (1500m) and CS4 (5km). The SN-LES results presented below (in Section 3.0) are inclusive of CS1, CS2 and CS3, but do not consider the larger mesoscale structure CS4 (seen as 3-D open cells in satellite imagery; see Fig. 2 in ZBAS).

The CS1 represents the onset CS that is literally attached at the air-lake interface to a similar structure that is at the top of the surface layer in the lake. The CS1 structures are embedded within the larger pattern of CS2 structures (see Fig. 8 in ZBAS). The air-lake interface should not be viewed as a discontinuity, but one that literally "interfaces" the *same* geometric pattern in both the air and water. The structures in the water can best be described as Langmuir circulations, which in the most general sense can be manifested as 2-D or 3-D patterns, or even chains of 2-D and 3-D geometry. Traditionally, Langmuir circulations are commonly viewed as 2-D rolls, driven by the surface stress vector,

*Corresponding author address: Ernest M. Agee, Purdue University, Dept. of Earth & Atmospheric Sciences, West Lafayette, IN 47907-2051; e-mail: agee@purdue.edu.

manifesting patterns of "wind rows" on the water surface. Nonlinear effects, however, are now recognized as having the ability to alter this simplistic pattern, and can manifest combinations of 2-D and 3-D structures that are just as complicated as those seen in the atmospheric PBL. The role of the wind field in developing dynamical structures in *both* the air and water surface layers has been studied extensively, but the effect of strong surface heat flux at the air-water interface during CAO events has not been properly considered. The effect of strong winds is typically viewed as "forcing" 2-D structures in both the air and the water; however, the effect of strong heat flux can *three-dimensionalize* the flow. This concept is best illustrated when viewing the deformation of the lake or ocean surface through the use of Synthetic Aperture Radar (SAR). The ZBAS paper (see their Fig. 13) shows SAR imagery of 2-D ocean surface deformations for strong winds and no heat flux, however, a pattern of 3-D ocean surface deformation is seen for conditions of both strong wind and large heat flux at the ocean-air interface. Heat flux can overcome the roll structure, in spite of strong winds, resulting in a 3-D cellular pattern of ocean surface deformation. The geometric structure of the ocean (or lake) surface clearly becomes a bottom boundary condition for modeling atmospheric flows and a top boundary condition for modeling the ocean (or lake) surface layer. This defining effect or structure can be viewed as a footprint of the participating physical mechanisms. In other words, the air affects the water surface layer and vice versa (a concept that is all too familiar, but not limited, to climate modelers). In a similar manner to the discovery offered by SAR imagery, is the Wisconsin lidar steam fog patterns for the Lake-ICE CAO event in this study (see Mayor and Eloranta 2001). Their Fig. 8 shows 3-D structure in the lidar observations of the steam fog pattern attached to the air-lake interface (also see their Fig. 9). Although larger CS length scales can grow within the convective PBL, the fundamental onset mode (CS1) is literally "rooted" to the water. Presented only as a conceptual physical model in this paper, a completely coupled air-lake model that produces both CS in the PBL and Langmuir circulations in the water is warranted.

3. SN-LES RESULTS FOR LAKE-ICE CAO

The SN-LES model has been run for the 13 January 1998 CAO over Lake Michigan. The clear-air version of the SN-LES code was deployed, since the focus of the convective simulation was in the CFP region between the Wisconsin shoreline and the cloud-topped PBL. The smaller CS length scales are of interest, beginning with the CS1 microscale structure at the air-lake interface and extending to the larger CS2 and CS3 length scales (previously defined). The grid resolution adopted is 10m x 10m x 10m, with a domain size of 2km x 2km (horizontal) and 1km (vertical). The model was initialized using the ISS Lake-ICE data, collected at Sheboygan at 1630 UTC 13 January 1998. This time was chosen to be as close as possible to the lidar VIL imagery (discussed later). The initial inversion height was set at 450m, and the horizontal surface winds were

$u = 13 \text{ ms}^{-1}$ and $v = -10 \text{ ms}^{-1}$. The basic state mixed layer was 252.5°K, and the initial surface heat flux was 500 Wm^{-2} . The model was run for 12,000 time steps, with a simulation time of 4400s (or about ten large eddy turnover times). Figure 1 shows the vertical profile of potential temperature (θ) for selected run times out to 12,000 time steps (~4400s or 10 large eddy turnover times). The convective PBL is characterized by a well-mixed layer up to 750m, with a superadiabatic surface layer from the air-lake interface up to 125m. These results agree reasonably well with MTE and ZBAS, except the latter was for only 6000 time steps. Also, the MTE LES results were for 15m x 15m x 15m, compared to 10m x 10m x 10m for ZBAS and in this study. The MTE LES domain was 11.68km x 1.8 km x 1km, which employed open boundary conditions and a domain that was nearly equal over land and water. The domain for both ZBAS and this study was placed over the CFP region of the lake, with periodic boundary conditions.

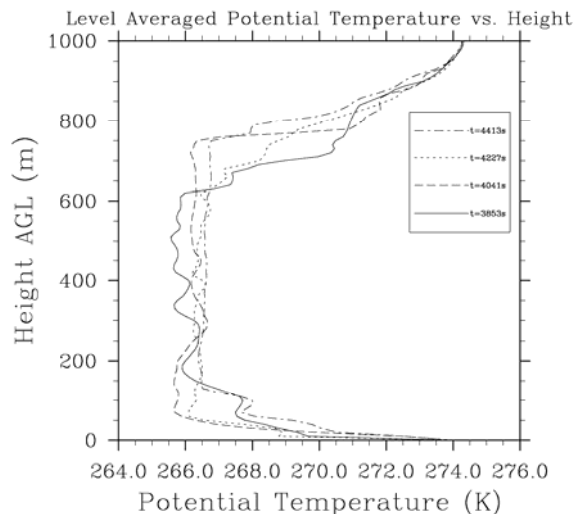


Figure 1. Vertical profile of horizontally averaged potential temperature for SN-LES for selected times that show quasi-steady state ($t = 4413\text{s}$ corresponds to about 10 large eddy turnover times).

As noted in the earlier discussion, this study has focused more specifically on the occurrence of multiple scales of coherent structures, and their apparent role in the development of the convective PBL. Coherent structures observed in Lake-ICE were previously defined as CS1, CS2, CS3 and CS4 (with appropriate length scales specified). The CS obtained in this study using the SN-LES model are now labeled, respectively as CSM1, CSM2, CSM3, CSM4 and CSM5. Figure 2a shows the quasi-steady planform of vertical velocity at $Z = 5\text{m}$ (above the lake) and appears to have primarily 3-D open cellular structures of varying length scales. The largest, somewhat irregular, open cells are even more apparent at higher levels (e.g., see Fig. 3). Smaller scale structures, however, are much more evident near the lake surface, as seen in Fig. 2b, which shows the same vertical velocity planform except for a different

color scheme to enhance the presence of the smaller scales. The box region in Fig. 2b shows an area that contains several of the smallest irregular open cells with diameters of approximately 50m to 100m, and these are defined as CSM1 structures. Also evident in both Figs. 2a and 2b are larger (intermediate size) open cells of about 200m, defined as CSM2. The same box region in Fig. 2a shows the CSM2 structures (that contain the embedded CSM1 structures). These two scales from the LES are analogous to CS1 and CS2 observed in Lake-ICE. The largest open cells can now be seen at $Z = 15\text{m}$ in Fig. 3, with diameters of about 500m (defined as CSM3). All of these results should be compared to the patterns seen in the lidar imagery and cloud photography shown in Figs. 8 and 9 in ZBAS.

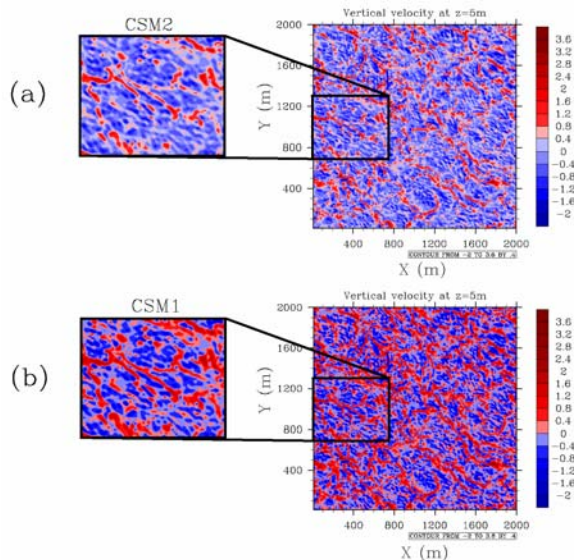


Figure 2. Horizontal planform of vertical velocity at $Z = 5\text{m}$ above lake surface. (a) The more prominent 3-D coherent structures (CSM2) are evident across the domain and, for example, can be readily identified in box region (which shows 3 or 4 irregular open cells). (b) Same as part (a) except the smaller scale structure (CSM1) are more evident in the box region due to a color enhancement scheme.

Next, it is shown that the 3-D structures (near the lake surface) give way to 2-D structures at higher levels. Figure 4 shows the horizontal planform of vertical velocity at $Z = 105\text{m}$, and these 2-D structures are defined as CSM4. These rolls are oriented parallel with the wind field, and have characteristic horizontal spacing of about 1km (also see MTE and ZBAS). This length scale (and 2-D structure) is comparable to that observed from the analysis of the lidar wind observations presented in ZBAS (see their Fig. 11). Thus CSM4 is comparable to CS3. It is also interesting to note that this larger 2-D coherent structure was faintly present in Figs. 2a, 2b and Fig. 3. It should be noted that all LES products presented at the higher levels (i.e., $Z > 100\text{m}$) are now "tiled." This is simply taking a single piece of "tile" that is 2km x 2km (the original domain) and creating a 4-piece array of tile that is 4km x 4km.

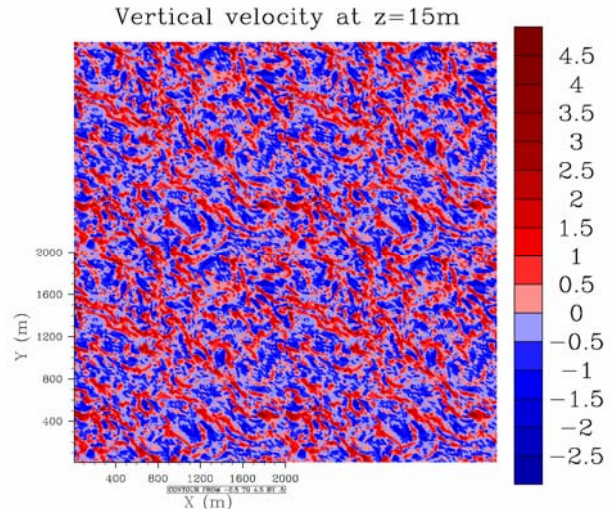


Figure 3. Same as Fig. 2a, except at $Z = 15\text{m}$ above lake surface. The box region shows the largest 3-D open cells (CSM3).

One can take this approach, since periodic boundary conditions are employed, thus allowing better visualization of the larger coherent structures (and this approach cannot be done to identify structures larger than the domain). Moving yet to a higher level, $Z = 245\text{m}$, Fig. 5 shows further strengthening of CSM4, as well as the emergence of a new 3-D structure defined as CSM5. This 3-D structure is even better defined in

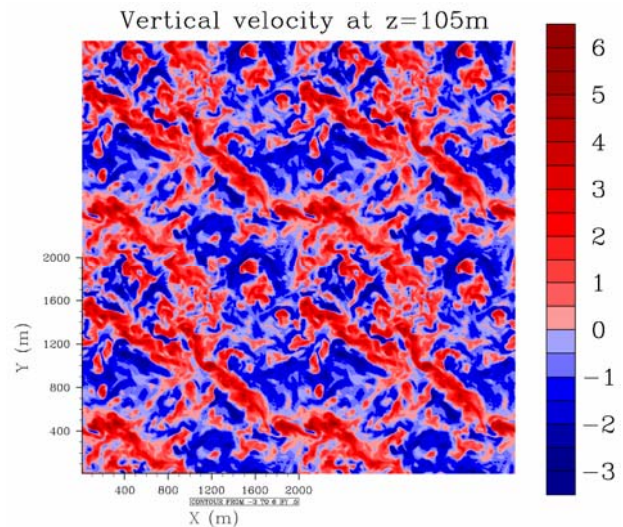


Figure 4. Horizontal planform of vertical velocity for a 4-tile array at $Z = 105\text{m}$. The labeled axes identify a single piece of domain "tile." The 2-D CSM4 structures are evident (with some evidence of "3-D" hexagonal cells or CSM5).

Fig. 6 at $Z = 325\text{m}$, although it can be traced to lower levels. Both CSM4 and CSM5 are of comparable length scale, about 1 km. Figure 7 shows CSM5 at $Z = 565\text{m}$, and this 3-D structure dominates the remainder of the upper portion of the mixed layer. This larger 3-D

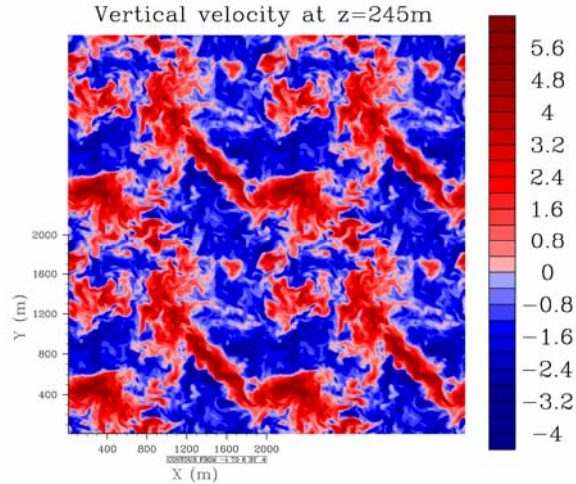


Figure 5. Same as Fig. 4, except at $Z = 245\text{m}$.

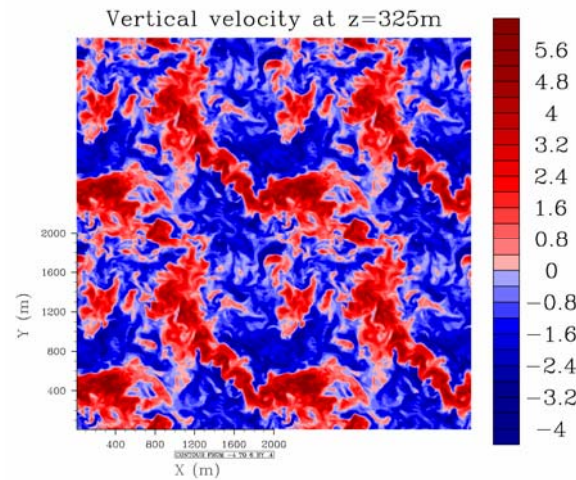


Figure 6. Same as Fig. 4, except at $Z = 325\text{m}$.

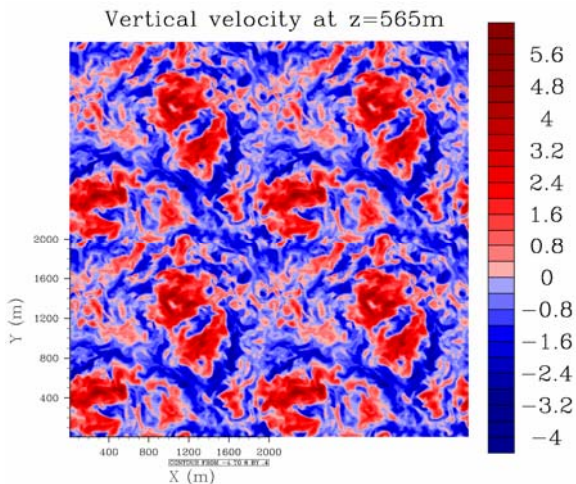


Figure 7. Same as Fig.4, except at $Z = 565\text{m}$. At this level, the 3-D CS pattern (CSM5) fully dominates the flow field.

structure was not found in MTE, as discussed in their paper. It is important to note at this time that the SN-LES runs here for about 10 large eddy turnover times, and also for a dry version of the model (thus no clouds). In the real case, the CFP length corresponds to a real time of about one large eddy turnover for the CAO wind field. As noted earlier, the LES did capture the smaller CS that were observed in Lake-ICE, but due to the run time, the LES did show the emergence of the larger 2-D and 3-D structures. This could be viewed as the type of CS that one might expect farther out over the lake and does correspond to structures seen in the cloud-topped PBL (although the LES model was dry). Again, one can refer to the satellite imagery in ZBAS (see their Fig. 2).

4. SUMMARY AND CONCLUSIONS

The SN-LES has been successfully implemented to study the Lake-ICE CAO of 13 January 1998. This was the third LES model to examine this event (the other two being the Tripoli and Sorbjan LES models). It is important that different LES models simulate the same convective PBL development, as noted by Siebesma et al. (2003). In fact, that study of LES for a given set of trade wind cumuli observations examined an ensemble of 10 different LES codes. Results obtained in this study showed the emergence of five different CS that coexist through much of the convective PBL. The three smallest CS were best defined in the surface layer and their geometry was 3-D, in spite of the strong surface winds. The smallest two scales, CSM1 and CSM2, corresponded well to the CS1 and CS2 scales observed in Lake-ICE. The largest 3-D cells in the surface boundary layer did not readily correspond to any observed Lake-ICE CS. The CSM4 2-D CS was strongly present in the lower half of the mixed layer, and was viewed as comparable to the lidar wind field 2-D pattern reported in ZBAS. This CSM4 is comparable to CS3. The middle and upper portions of the mixed layer were dominated by a 3-D cellular pattern (CSM5), also of comparable size to CSM4 (about 1km). Both the 2-D and 3-D CS were traceable to lower levels, including the surface boundary layer. The CSM5 3-D pattern in the upper half of the mixed layer was not found in MTE and ZBAS, but was supported by both lidar and satellite imagery.

Finally, some general comments and insight into the strengths and weaknesses of LES seem warranted. As noted by Lesieur et al. (2005), LES does allow one to predict the dynamics of CS, however, all LES models of atmospheric flows are plagued by the inverse cascade of unpredictability. In fact, Lesieur (1997) has proposed reasonable defining criteria for two grades of LES (stopping short of a third definition for exact prediction). Again, as noted by Pope (2004), there is no right approach for modeling all scales of fluid motion; however, LES continues to be appropriate for studying the dynamics of the convective PBL. Heating from below is the principal mechanism that drives the motion, which is reasonably resolvable in current LES models.

5. ACKNOWLEDGEMENTS

The authors are grateful to Peter Sullivan at NCAR for graciously providing the LES code and for his assistance in its implementation. Gina Richey is acknowledged for assistance in manuscript preparation. This research is sponsored by NSF Grant ATM-0514674 awarded to Purdue University.

6. REFERENCES

- Agee, E. M., and A. Gluhovsky, 1999: LES model sensitivities to domains, grids, and large-eddy timescales. *J. Atmos. Sci.*, **56**, 599-604.
- Deardorff, J. W., 1970: A numerical study of three dimensional turbulent flow at large Reynolds numbers. *J. Fluid Mech.*, **42**, 453-461.
- , 1974: Three-dimensional numerical study of turbulence in an entraining mixed layer. *Bound.-Layer Meteor.*, **7**, 199-226.
- , 1980: Cloud top entrainment instability. *J. Atmos. Sci.*, **37**, 131-147.
- Lesieur, M., 1997: *Turbulence in Fluids (Fluid Mechanics and Its Applications)*. Kluwer Academic Publishers, 515 pp.
- , O. Métais, and P. Comte, 2005: *Large-Eddy Simulations of Turbulence*. Cambridge University Press, 232 pp.
- Lilly, D. K., 1967: The representation of small-scale turbulence in numerical simulation experiments, *Proc. IBM Scientific Computing Symposium on Environmental Sciences*, White Plains, N.Y., 195.
- Mason, P. 1989: Large-eddy simulation of the convective atmospheric boundary-layer. *J. Atmos. Sci.*, **46**, 1492-1516.
- Mayor, S. D., and E. W. Eloranta, 2001: Two-dimensional vector wind fields from volume imaging lidar data. *J. Appl. Meteor.*, **40**, 1331-1346.
- , G. J. Tripoli, and E. W. Eloranta, 2003: Evaluating large-eddy simulations using volume imaging lidar data. *Mon. Wea. Rev.*, **131**, 1428-1453.
- Moeng, C.-H., 1984: A large-eddy simulation model for the study of planetary boundary layer turbulence. *J. Atmos. Sci.*, **41**, 2052-2062.
- , 1986: Large-eddy simulation of a stratus-topped boundary layer. Part I: Structure and budgets. *J. Atmos. Sci.*, **43**, 2886-2900.
- , and J. C. Wyngaard, 1988: Spectral analysis of large-eddy simulations of the convective boundary layer. *J. Atmos. Sci.*, **45**, 3573-3587.
- , and P. P. Sullivan, 1994: A comparison of shear- and buoyancy-driven planetary boundary layer flows. *J. Atmos. Sci.*, **51**, 999-1022.
- Nieuwstadt, F. T. M., P. J. Mason, C.-H. Moeng, and U. Schumann, 1991: Large-eddy simulation of convective boundary-layer: A comparison of four computer codes. *Turbulent Shear Flows*, F. Durst et al., Eds., Vol. 8, Springer-Verlag, 343-367.
- Pope, S. B., 2004: Ten questions concerning the large-eddy simulation of turbulent flows. *New Journal of Physics*, **6**, 1-24.
- Rao, G.-S., and E. M. Agee, 1996: Large eddy simulation of turbulent flow in a marine convective boundary layer with snow. *J. Atmos. Sci.*, **53**, 86-100.
- Schumann, U., 1975: Subgrid-scale model for finite difference simulation of turbulent flows in plane channels and annuli. *Comput. Phys.*, **18**, 376-404.
- , 1993: Large eddy simulation of turbulent convection over flat and wavy surfaces. *Large Eddy Simulation of Complex Engineering and Geophysical Flows*, B. Galperin and S. A. Orszag, Eds., Cambridge University Press, 399-421.
- Siebesma, A. P., C. S. Bretherton, A. Brown, A. Chlond, J. Cuxart, P. G. Duynkerke, H. Jiang, M. Khairoutdinov, D. Lewellen, C.-H. Moeng, E. Sanchez, B. Stevens, and D. E. Stevens, 2003: A large eddy simulation intercomparison study of shallow cumulus convection. *J. Atmos. Sci.*, **60**, 1201-1219.
- Smagorinsky, J., 1963: General circulation experiments with the primitive equations. *Mon. Wea. Rev.*, **91**, 99-164.
- Sorbjan, Z., 2004: Large-eddy simulations of the baroclinic mixed layer. *Bound.-Layer Meteor.*, **112**, 57-80.
- Tripoli, G. J., 1992: A nonhydrostatic mesoscale model designed to simulate scale interaction. *Mon. Wea. Rev.*, **120**, 1342-1359.
- Zurn-Birkhimer, S., E. M. Agee, and Z. Sorbjan, 2005: Convective structures in cold air outbreak over Lake Michigan during Lake-ICE. *J. Atmos. Sci.*, **62**, 2414-2432.